Subpixel Classification of Bald Cypress and Tupelo Gum Trees in Thematic Mapper Imagery

Robert L. Huguenin, Mark A. Karaska, Donald Van Blaricom, and John R. Jensen

Abstract

A subpixel spectral analytical process was used to classify Bald Cypress and Tupelo Gum wetland in Landsat Thematic Mapper imagery in Georgia and South Carolina. The subpixel process enabled the detection of Cypress and Tupelo trees in mixed pixels. Two-hundred pixels were field verified for each tree species to independently measure errors of omission and commission. The cypress total accuracy was 89 percent and the tupelo total accuracy was 91 percent. Field investigations revealed that both cypress and tupelo trees were successfully classified when they occurred both as pure stands and when mixed with other tree species and water. In a comparison with traditional classification techniques (ISODATA clustering, maximum likelihood, and minimum distance) the subpixel classification of cypress and tupelo yielded improved results. Large areas of wetland where cypress was heavily mixed with other tree species were correctly classified by the subpixel process and not classified by the traditional classifiers.

Introduction

Forested wetland ecosystems are increasingly under pressure for conversion to commercial (e.g., timber extraction, agriculture, hotels, marinas) and residential land use (single- and multiple-family dwellings). The type and geographic location of wetland within the parcels of interest must be identified and delineated to determine if the land should be developed. This involves intensive field work, and, for large parcels, it is often impractical to manually survey the entire area. To reduce the extent of the field work, aerial infrared photography and digital remote sensing imagery are often used to locate overstory indicator species that can be used to delineate upland to wetland gradients. There has been significantly more success using aerial infrared photography than digital remote sensing imagery for this application. The aerial infrared photographs are generally acquired at large enough scales to resolve individual tree crowns, allowing indicator wetland species to be detected based on their color, spatial, and textural characteristics.

Scientists have been trying to extract wetland information from coarse spatial resolution digital Landsat Multispectral Scanner (MSS) imagery (80 x 80 m) since 1972, Landsat Thematic Mapper (TM) imagery (30 x 30 m) since 1982, and SPOT multispectral data (20 x 20 m) since 1986 (Hodgson *et al.*, 1988; Jensen *et al.*, 1995). Investigators have successfully inventoried large monospecific stands of wetland plant species using pattern recognition image classification techniques. However, heterogeneous wetlands containing several plant species plus standing water often cannot be classified correctly using the coarse spatial resolution remote sensor data. This is because the traditional per-pixel classification algorithms cannot disaggregate the individual materials of interest within the instantaneous field-of-view (IFOV) of the sensor system.

For example, consider the hypothetical TM pixel data shown in Figure 1 that contains approximately equal percentages of cypress (33 percent), tupelo (33 percent), and water (33 percent). Table 1 and Figure 1a reveal that the integrated digital number (DN) value output of this pixel in six bands (TM thermal Band 6 is excluded) is substantially different from any of the spectral reflectance spectra associated with "pure" cypress, "pure" tupelo, and "pure" water land cover. The integrated "mixed pixel" frequently causes classification confusion, and it can prohibit the classification of individual materials of interest because the mixed pixel composite spectral signature is unlike the spectral signature of the individual surface materials occurring as subpixel components.

Individual wetland plant species and surface materials that occur as subpixel components in TM mixed pixels have the potential to be spectrally resolved and classified using subpixel processing techniques that can distinguish surface materials smaller than the spatial resolution of the sensor.

Subpixel Processing

Remote sensing image analysts typically deal with the mixed pixel problem by labeling "mixed pixels" with "mixed labels." For example, a pixel containing 70 percent cypress and 30 percent tupelo may be labeled "mixed cypress-tupelo" because there has been no mechanism for extracting information about the proportion of individual materials of interest within pixels using traditional per-pixel classification logic. The traditional classifiers have generally performed well for classifying large, monospecific stands of tree species, but they have not been successful in the identification of the proportions of several materials of interest found within the IFOV of a sensor

R.L. Huguenin and M.A. Karaska are with Applied Analysis Inc., 46 Manning Road, Suite 201 Billerica, MA 01821 (aai @discover-aai.com).

D. Van Blaricom is with the Strom Thurmond Institute, Clemson University, Clemson, SC 29634.

J.R. Jensen is with the Department of Geography, University of South Carolina, Columbia, SC 29208 (johnj@garnet.cla.sc.edu).

Photogrammetric Engineering & Remote Sensing, Vol. 63, No. 6, June 1997, pp. 717–725.

0099-1112/97/6306-717$3.00/0

system (Jensen *et al.*, 1995). An approach for doing this is *subpixel processing*, defined as the search for specific materials of interest from within a pixel's mixed multispectral image digital number spectrum. Subpixel processing does not provide information on where the material of interest occurs within the pixel. It does provide important information on the relative proportion of the material of interest found within a pixel (e.g., this pixel contains 77 percent cypress).

This paper describes a subpixel image classification process.[1] It is demonstrated by classifying wetland Bald Cypress (*Taxodium distichum*) and Tupelo Gum (*Nyssa aquatica*) in TM imagery of South Carolina and Georgia study areas. The results of an accuracy assessment involving a Global Positioning System (GPS) field verification of 200 pixel locations for each tree species is presented. The subpixel classification process is also compared with more traditional image classification algorithms.

How the Subpixel Processor Works

The general subpixel processing steps are summarized in Figure 2. Unrectified multispectral remote sensor data are processed to remove atmospheric radiance and attenuation effects. Then, a signature is derived for a material of interest (MOI). Each pixel is then classified as to its fraction of material of interest present. For example, if the MOI is cypress, each pixel in the scene will contain a number from 0 to 1.0 identifying the proportion of cypress within the pixel. Information about the various stages are presented below.

To address the mixed pixel problem, the subpixel processor assumes that each image pixel, P_m, contains some fraction, f_m, of the material of interest, M, (e.g., cypress), and the remainder, $1 - f_m$, contains other background materials, B_m; i.e.,

$$P_m = (f_m \times M) + [(1 - f_m) \times B_m]. \quad (1)$$

[1]The Applied Analysis Spectral Analytical Process (AASAP) is an ERDAS Imagine module.

TABLE 1. HYPOTHETICAL LANDSAT THEMATIC MAPPER DATA OF FIVE 30- BY 30-M PIXELS CONTAINING, RESPECTIVELY, PURE CYPRESS, PURE TUPELO, PURE WATER, AND EQUAL PROPORTIONS OF CYPRESS, TUPELO, AND WATER.

TM Bands	Cypress (pure)	Tupelo (pure)	Water (pure)	Tupelo (33%) + Water (33%)	Cypress (33%) + Tupelo (33%) + Water (33%)
1	21	27	24	17	24
2	18	15	21	12	18
3	33	27	12	13	24
4	48	42	9	17	33
5	42	33	6	13	27
7	39	27	3	10	33

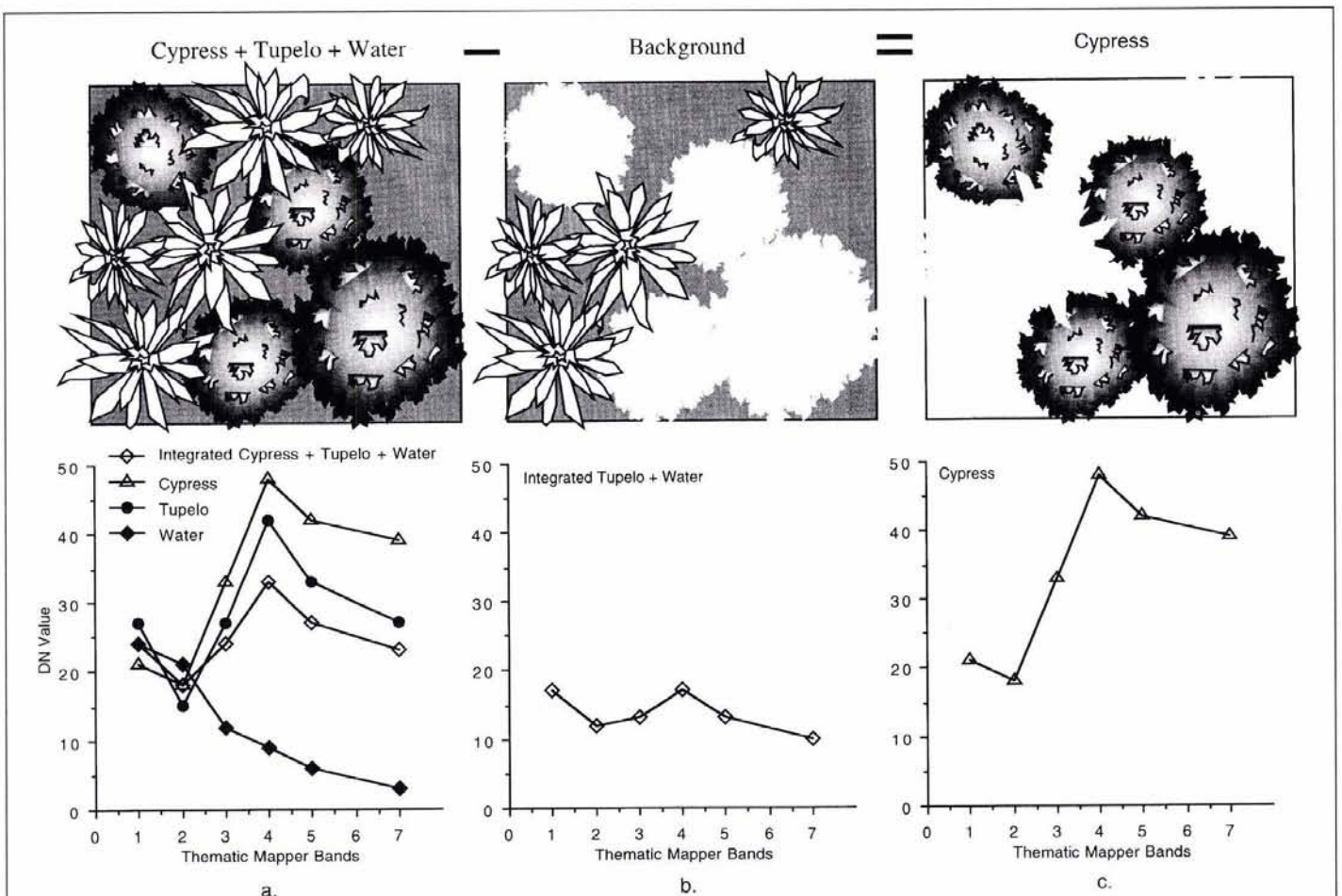

Figure 1. A schematic diagram of how a material of interest (MOI) (cypress in this example) is extracted using subpixel processing from a hypothetical Landsat TM 30- by 30-m mixed pixel containing equal proportions of cypress, tupelo, and water. (a) The integrated spectrum for the pixel bears little resemblance to the pure spectrum of any of its constituents. (b) The background reflectance spectrum is identified. (c) The background reflectance spectrum is subtracted from the original integrated spectrum, leaving only information about the proportion of the material of interest, cypress, within the pixel.

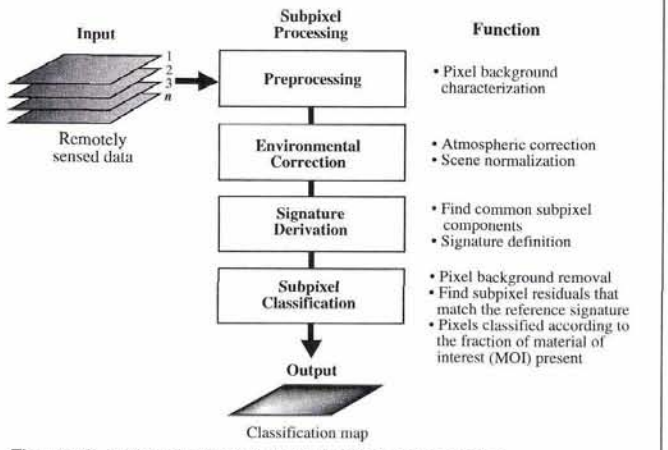

Figure 2. Typical stages in subpixel processing.

In Figure 1, if cypress were the material of interest (M), then f_m would equal 0.33 and the remainder of the background surface cover materials (B_m) would be $(1 - f_m) = 0.67$. In Equation 1, M is a single specified material of interest such as cypress. The value B_m in Equation 1 refers to all of the other materials in the pixel, treated as a single combined set of "background" materials. The value f_m is an areal fraction. Equation 1 assumes that M is invariant from pixel to pixel, while P_m, f_m, and B_m vary from pixel to pixel. In this paper we report results for two materials, cypress and tupelo. It is important to remember that each material of interest was searched for independently, i.e., in one analysis M was cypress and in another analysis M was tupelo.

For the applications reported here, M and B_m were assumed to be optically thick (no transmittance through the material) in at least one of the spectral bands. Therefore, the radiant contributions from M and B_m were assumed to be approximately linearly additive in spectral bands, n: i.e.,

$$R_m[n] = (k_m[n] \times T[n]) + ((1 - k_m[n]) \times L_m[n]) \quad (2)$$

where, $R_m[n]$, $T[n]$, and $L_m[n]$ are the radiances from, P_m, M, and B_m in pixel m and band n, respectively. $k_m[n]$ is the radiant fraction contributed by $T[n]$ in pixel m and band n. Note that the radiant fraction, $k_m[n]$, can vary from band to band, because the radiant contrast between the material of interest and the background can vary from band to band. In bands for which there is little radiant contrast between the material of interest and the background, $k_m[n]$ will be approximately equal to f_m. In bands for which the background radiance is significantly lower than that for the material of interest, then $k_m[n]$ will be greater than f_m.

The subpixel process detects the material of interest in a pixel under investigation by subtracting fractions of candidate background spectra, and then identifying the background and fraction that produces the residual spectrum that most closely matches the spectrum for the material of interest. For each candidate background, residuals are computed that produce the best spectral match to the spectrum for the material of interest. The residual, $T_m[n]$, is calculated according to the expression

$$T_m[n] = (R_m - ((1 - k_m) \times L_m[n])) / k_m \quad (3)$$

where k_m is the fraction of the material of interest in the pixel, and $(1 - k_m)$ is the fraction of background, $L_m[n]$, removed from the pixel radiant spectrum, $R_m[n]$. The degree of spectral match between the residual $T_m[n]$ and the signature spectrum $T[n]$ is computed by the expression

$$f = \sum_{n=1}^{N} (T_m[n] - T[n])^2 / N \quad (4)$$

where N is the number of image planes. The set of candidate backgrounds, $L_m[n]$, is unique for each pixel under investigation. It is assumed that the background for the pixel under test can be represented by other pixels in the scene. The set of candidate backgrounds is independently selected for each pixel under investigation, because the background in each pixel can be unique. Selected candidates may include local neighbors to the pixel under test, as well as pixels from elsewhere in the scene. For the application here, local neighbors were not generally selected, because those pixels frequently also contained significant fractions of the material of interest.

The residual spectrum found using Equation 3 is considered valid when all of its values are greater than zero. An invalid residual indicates that a candidate background is not representative of the actual background in the pixel under investigation. If all of the candidate backgrounds fail to generate a valid residual, then the pixel under test does not contain a detectable amount of the material of interest.

The residuals that are valid are next screened according to the boundaries of a feature space, which is defined during the signature derivation process described below. If the residual passes the screen, then the reported fraction is stored in the appropriate row by column location in an output image. The output image thus takes the form of a fraction plane for the material of interest.

Environmental Correction Process

To use Equation 2 to search for the materials of interest, the raw digital numbers for pixel m, $DN_m[n]$, are corrected to remove the atmospherically scattered solar radiance component and the sensor offset factors. An environmental correction module uses sampled pixels from the scene being processed to derive a correction factor, ARAD[n], that is subtracted from $DN_m[n]$ to provide the requisite proportionality to $R_m[n]$ in Equation 2. The proportionality factor includes the sensor gain factor and the atmospheric attenuation of the incident and reflected solar and sky radiance in each spectral band, n. These latter factors plus the incident solar and sky radiance terms are included in a second factor calculated by the module, SF[n]. SF[n] is only used for scene-to-scene applications, i.e., applications in which a signature developed in one scene is used in another scene.

The ARAD[n] factor used for this study was automatically derived by the process using subpixel detection of pseudo-calibration materials in the scene. These are materials that are indigenous to the scene and that can be used in a manner similar to deployed calibration panels. The principal difference is that the indigenous materials are rarely usable as calibration materials across all spectral bands. To compensate for this limitation, AASAP blends the spectra from several of these pseudo-calibration materials to form the desired calibration spectra.

The pseudo-calibration materials used to calculate ARAD[n] are the darkest materials in the scene, such as deep clear water and shadowed terrain materials. The contributions of these dark surface materials to the overall pixel radiance are generally minimal, allowing the atmospherically scattered solar radiance component to dominate. The use of dark water and shadowed terrain pixels to remove atmospherically scattered solar radiance from scene pixels is common practice in multispectral image analysis. The success has been mixed, however, because water pixels and shadowed terrain pixels often contain significant unwanted surface reflectance contributions, such as reflected sky radiance and sun glints in water pixels and solar illuminated terrain in predominantly shadowed pixels. By using the subpixel

process, the unwanted glints and illuminated terrain contributions are effectively suppressed, allowing a generally more accurate atmospheric radiance spectrum to be derived.

The ARAD[n] factor is scene-specific, and it is assumed to be invariant from pixel to pixel within the scene. Pixel-to-pixel variations of haze and other environmental factors are not directly compensated for by ARAD[n]. Although only ARAD[n] was used for the in-scene application reported here, both ARAD[n] and SF[n] were automatically calculated and stored with the signature to allow the signature to be used for scene-to-scene applications.

Obtaining the Training Signature of the Material of Interest

The signature of the material of interest consists of a signature spectrum and a non-parametric feature space. The signature spectrum is the equivalent of a spectrum of an image pixel comprised entirely of the material of interest. AASAP uses the signature spectrum to (1) control the selection of candidate backgrounds for removal from each image pixel, and (2) control the determination of what fractions of the background to remove from the pixel. The non-parametric feature space is used to filter the residuals created by removal of the background during the classification process.

A signature derivation module derives the signature spectrum and feature space from user-specified training pixels and parameter values. The training set consists of image pixels that were estimated to contain a relatively consistent amount of the material of interest. For this application, each of the training set pixels was estimated to contain >90 percent cypress or tupelo. The user-specified parameter values include the estimated fraction of the material of interest in the training set pixels (mean material pixel fraction) and the estimated probability that any given training set pixel actually contains the material of interest (confidence factor). For both the cypress and tupelo, the material pixel fractions and confidence factors were 0.90.

The subpixel processor uses the specified material pixel fraction to determine the amount of background to remove from each training set pixel. The confidence factor is used to determine how many of the training set pixels need to be included and how many can be excluded during the signature derivation process. The residuals (after background removal) derived from the included pixels are combined to create the signature spectrum.

A multi-dimensional spectral feature space is created to set tolerances on the spectral variability of the residuals (detected during classification) relative to the signature spectrum. The variability can arise from two principal sources, variations in the spectral properties of the material of interest and errors inherent in the background removal process. The resultant signature represents the material that was common to the set of training pixels at the specified material pixel fraction. This differs from traditional classifiers where the variance of the training set defines the range of materials included in the classification. The subpixel classifier does not simply accommodate the material variance of the training set pixels. Instead, it extracts the signature of the material that is common to the training set pixels. This has the advantage of allowing signatures of relatively specific materials of interest to be derived from mixed pixels, rather than deriving signatures of the mixture of materials in the training set. The signature spectrum, feature space, and environmental correction spectra are stored in a signature file.

Subpixel Processing in Relation to Other Approaches

The subpixel processing may provide a more robust discrimination than traditional per-pixel multispectral classifiers for pixels where the material of interest is mixed with other materials. It also provides more uniform performance away from the training sites. This is a consequence of the enhanced purity of reference signatures, discussed above. It is also a consequence of the background suppression capability used during classification. The spectral contribution of the background materials in the pixel can significantly distort the pixel spectrum from that of the material of interest. By suppressing these background contributions, discriminations can be maintained between spectrally similar materials even when the material of interest occupies only a small fraction of the pixel. Traditional multispectral classifiers are not able to directly suppress the background contributions. Instead, the variances imposed by the background materials are accommodated by the other classifiers. If too little variance is accommodated, then only the purest pixels can be discriminated. If too much variance is accommodated, then mixed pixels can be included in the classification but the discrimination sensitivity is reduced. The traditional classifiers have successfully performed species level discrimination for large contiguous stands. They have had mixed success, however, when the species were mixed with other terrain units.

The subpixel processing approach used for signature derivation and background suppression yields discrimination performance characteristics generally different from the Linear Mixing Model (LMM) (Adams *et al.*, 1986; Smith *et al.*, 1990). The LMM evaluates each pixel spectrum as a linear sum of a basic set of image end-member spectra. These typically include a "shade" spectrum and $n-2$ other scene-representative orthogonal spectra, where n is the number of sensor spectral bands. The end-member spectra include "background" end-members, such as bright soil, vegetation, and water, and "residual" end-members, such as concrete, tarmac, and roofing material. The background end-members are assumed to be in every image pixel, and the residual end-members are assumed to be in only some of the pixels. The output is typically presented in the form of fraction planes for each end-member spectrum, which give the derived fractions of each end-member spectrum for each pixel. A residual plane is also produced that gives the root-mean-square error of the fit for each image. The LMM has been most reliably used to classify pixels in a manner analogous to a principal components analysis. There have also been attempts to use the LMM for subpixel analysis by either substituting the material-of-interest spectrum for one of the residual end-member spectra, or by comparing the error spectrum to the material-of-interest spectrum. The LMM can produce reasonable subpixel results when the material of interest has a spectrum that is both orthogonal to the other end-member spectra and unique in the scene. The LMM can classify subpixel occurrences of shade, soil, or scene vegetation but it is generally not appropriate for detecting subpixel occurrences of specific vegetative species (Smith *et al.*, 1990).

The non-parametric AASAP subpixel process also yields results different from those produced using fuzzy set classification logic (Wang, 1990a; Wang, 1990b; Jensen, 1996). Fuzzy classification also yields subpixel "membership grade" information (i.e., a pixel might have a fuzzy set membership grade value of 0.7 cypress, 0.2 tupelo, and 0.1 water). However, it arrives at the membership grade statistics using supervised fuzzy set maximum-likelihood or fuzzy c-means clustering logic, and the results are not the same as the subpixel processing described here. Unlike AASAP, both the LMM and the fuzzy set logic assume that the overall composition of each pixel is constrained to be some combination of the defined image classes (or end-members for LMM).

Application of Subpixel Processing to Discriminate Cypress and Tupelo Materials of Interest in Landsat Thematic Mapper Imagery

The subpixel processing logic was tested on forested wetland study areas in South Carolina and Georgia using Landsat Thematic Mapper data.

Remotely Sensed Data

Landsat TM imagery obtained on 4 May 1992, after spring leaf-out, was analyzed. Four study areas from within the Landsat TM scene were analyzed (Figure 3). Two 150- by 150-pixel areas were used for signature training and classification refinement. The two training areas were processed to detect the locations of individual cypress and tupelo trees. In addition, two 256- by 256-pixel test areas were classified using the subpixel processor.

Low altitude color infrared (CIR) aerial photography was obtained at a nominal scale of 1:7,000 and 1:22,500 for the two training areas 14 and 15 days after the TM overpass. Large stands of cypress and tupelo, and in some cases individual tree crowns, could be identified in the 1:7,000-scale photographs. National Aerial Photography Program CIR aerial photographs (1:40,000 scale) were used to analyze regions of the study area outside the two training areas.

In Situ Field Data Collection for Training and Error Assessment

In situ field sampling was conducted to

(1) identify pure, homogeneous stands of cypress and tupelo for signature training;
(2) identify locations of cypress trees mixed with other tree species, and tupelo trees mixed with other tree species, for classification refinement; and
(3) measure errors of omission and commission in the accuracy assessment phase of the project.

Sampling was restricted to areas that were accessible by foot. However, due to an exceptionally dry field season (summer 1993), many deep wetland areas that normally are inaccessible by foot were accessible. The locations of TM pixels were found in the field using a TM pixel grid that was registered and overlaid on the 1:7,000-scale CIR photographs. A Global Positioning System (GPS) unit was used to identify ground control points for georeferencing and to acquire ground coordinates for training areas. Further discussion of the sampling methodology is found in Karaska *et al.* (1995).

Application of Subpixel Processing to Extract Individual Specie Material-of-Interest Information

The Landsat TM scene was acquired with nearest-neighbor resampling, 30- by 30-m pixels, and spacecraft path orientation. Nearest-neighbor resampling is preferred over cubic convolution or bilinear interpolation resampling methods for subpixel processing because it minimizes spectral degradation. Resampling for geometric correction is minimized with spacecraft path oriented and 30- by 30-m pixel data. Preservation of the spectral relationships between pixels and band-to-band spectral relationships within a pixel increase the potential for subpixel spectral discrimination. Geometric correction of the imagery for cartographic and cosmetic purposes was performed with cubic convolution resampling *after* subpixel processing.

Georeferencing was required to associate the ground coordinates of training and accuracy assessment sites with the corresponding Landsat TM pixels. To avoid additional resampling of the TM imagery, the ground coordinates of these sites were plotted on a digitized base grid map. This map was geometrically registered to the TM image. To find the location of classified pixels in the field, another form of image registration was performed. The TM pixel grid was registered to the 1:7,000-scale CIR photographs and printed on transparencies for overlay on the photographs. The georeferenced TM image was not used for subpixel processing.

As previously discussed, the subpixel processing involved using one set of training pixels to develop the cypress spectral signature and one set to develop the tupelo spectral signature. Another set of training pixels was used to refine the classification. All training pixels and the classification

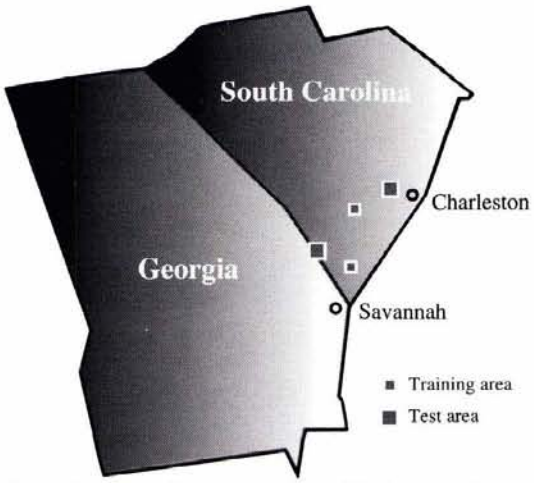

Figure 3. Approximate location of training and test study areas in South Carolina and Georgia.

evaluation and refinement occurred in the two 150- by 150-pixel training image areas. A signature can be developed for almost any material for which the analyst can identify a training set. The principal restrictions are that (1) the amount of material in the training pixels should exceed 20 percent of a pixel, (2) the material should have relatively unique and consistent spectral properties within the set of training pixels, and (3) each training pixel should contain approximately the same amount of the material of interest. The training set does not need to come from the same image being classified (Huguenin, 1994). After the spectral signatures were developed and refined, the remaining two test image areas were processed.

Known locations of relatively homogeneous stands of cypress and tupelo trees were used as training pixels. Fifty-one TM pixels of cypress from one training area were used. Field verification revealed that each of these pixels contained approximately 85 percent cypress. Seventy-two pixels of tupelo were used as training pixels. These pixels contained approximately 90 percent tupelo. These training pixels were used by AASAP to create a spectral signature for each species. The processor then evaluated each pixel in the image to determine if the pixel contained a subpixel spectral component that resembled the species spectral signature within a specified range of tolerances (refer to the subpixel classification phase in Figure 2). A variety of tolerances (thresholds) were evaluated in an iterative fashion until an optimal set of results were obtained.

Classification refinement involved evaluating the classification output from each iteration of the thresholds. These preliminary classification results were evaluated with the 1:7,000-scale aerial photographs, some field work, and the use of another set of training pixels. These training pixels were known to contain subpixel occurrences of the species. The classification results were refined until the maximum number of pixels containing some cypress (or tupelo) were correctly classified with the minimum number of incorrectly classified pixels.

Comparison with other Classification Algorithms

It is important to know how accurate the subpixel process is compared to traditional classification processes (e.g., unsupervised ISODATA clustering, supervised minimum distance, and supervised maximum likelihood). These algorithms were

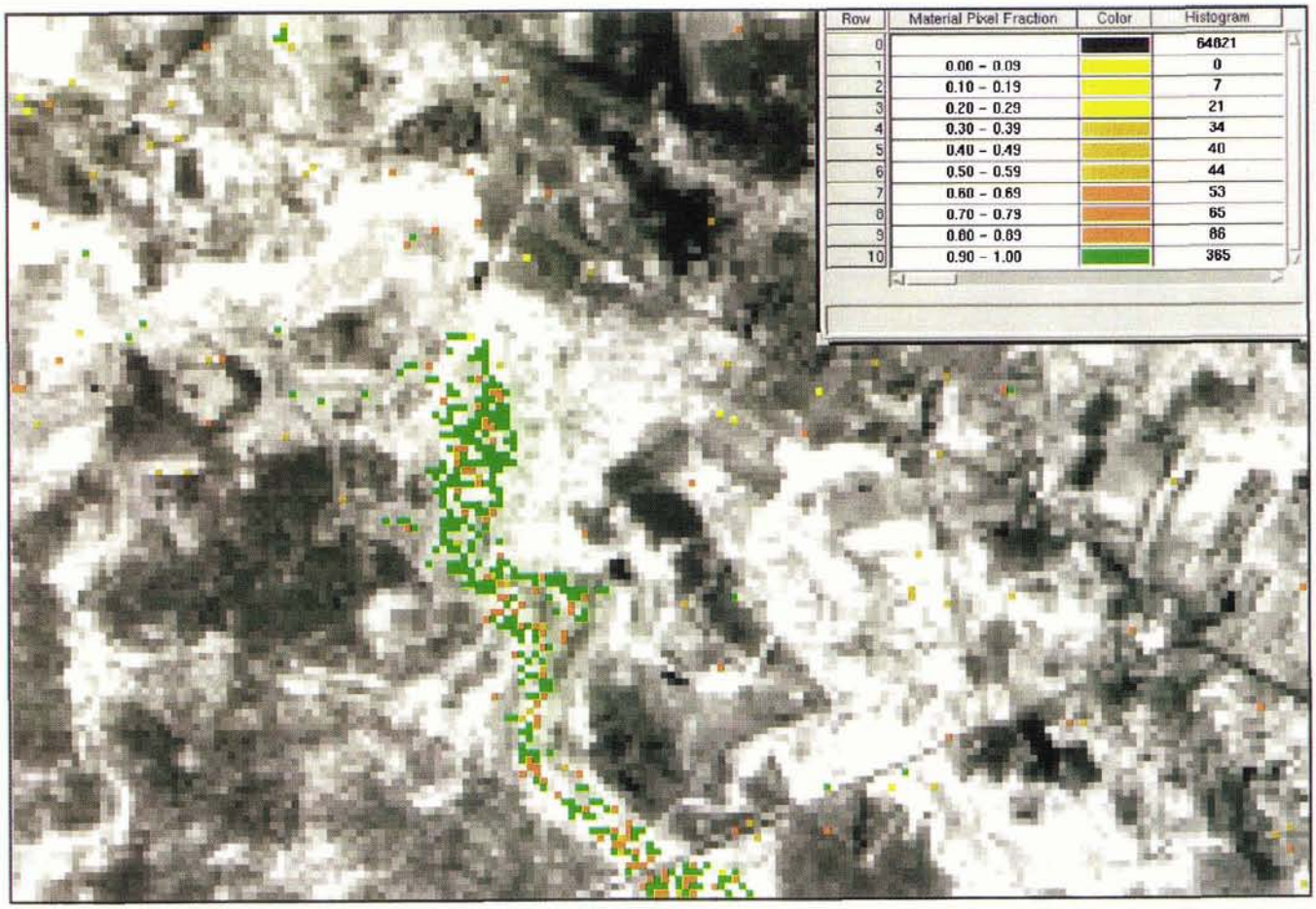

Plate 1. Tupelo land cover derived from subpixel processing of Landsat TM data for a region in South Carolina. Valuable information about the proportion of tupelo found within each pixel is summarized in the inset table and is color coded.

applied to the study area by an independent research team at Clemson University who were not involved with AASAP classification. The traditional classification process utilized the same resources available to the AASAP classification (the same nearest-neighbor resampled image, the CIR aerial photographs, and *in situ* field data). The Clemson University researchers were experienced at performing multispectral classifications and knew the study area well. The objective of the traditional classifications was to produce the most accurate classification of both cypress and tupelo trees using whichever traditional classifier worked best. The ISODATA, maximum-likelihood, and minimum-distance classifications used the same training and classification refinement areas (two 150- by 150-pixel areas) and classified the same four areas (the two 150- by 150-pixel training areas and the two 256- by 256-pixel test areas) as the AASAP classification.

The unsupervised ISODATA clustering process was eliminated from the comparison because it yielded inferior classification accuracy when compared with the supervised classifiers. ISODATA clusters were obtained that contained cypress and tupelo trees. Unfortunately, these clusters contained a large proportion of pixels that did not contain cypress or tupelo trees (a high level of commission error). The pure cypress and pure tupelo training pixels used by AASAP were used in both the maximum-likelihood and minimum-distance classifications. When using these pure training pixels, these classifiers did well in classifying other pixels of pure cypress and pure tupelo. However, most occurrences of tupelo and almost all the occurrences of cypress in this study area occurred in mixed pixels. To classify the pixels which contained cypress mixed with other wetland tree species and tupelo mixed with other tree species, training pixels containing these mixtures also had to be used. The overall best traditional classification result for cypress and tupelo was obtained using a mixed-pixel training set and optimizing the threshold on the minimum-distance classification. The identical accuracy assessment methods used to quantify the AASAP classification performance (100 pixels field verified for commission accuracy and 100 pixels field verified for omission accuracy for each species) were performed for the final minimum-distance classification. The accuracy assessment measures and the spatial distribution of the minimum-distance and AASAP classification were compared and evaluated.

Accuracy Assessment

The AASAP classifications yielded two output maps — one for cypress and one for tupelo. These maps contained material-of-interest fraction data in 10 percent increments about the amount of cypress or tupelo found in each pixel. The ideal subpixel processor error evaluation would compare (1) the remote sensing derived per-pixel fraction information (e.g., 60 percent in a pixel) with (2) *in situ* derived material-of-interest fraction data for the exact location on the ground (e.g., 70 percent). Unfortunately, it is difficult to quantify the

TABLE 2. ACCURACY ASSESSMENT RESULTS FOR THE CLASSIFICATION OF CYPRESS AND TUPELO USING SUBPIXEL PROCESSING.

Class	Commission Accuracy	Omission Accuracy	Total Species Accuracy
Cypress	95/100	82/100	89%
Tupelo	93/100	89/100	91%

material-of-interest pixel fraction information for native tree species in TM imagery because of the uncertainty in determining the precise location of the TM pixel on the ground, and the difficulty in quantifying the amount of the tree species present. Small errors in pixel position estimation significantly effect the assessment. Therefore, only the presence or absence of cypress or tupelo in a pixel was used in the error evaluation. All material-of-interest fraction information was ignored.[2]

For both the AASAP and minimum-distance classification results, random sampling techniques were used to select 200 locations that were field verified for the occurrence of cypress trees and 200 locations that were field verified for the occurrence of tupelo trees. For both cypress and tupelo, 100 pixel locations were field verified to measure errors of commission (approximately 25 locations in each of the four image areas), and 100 pixel locations were field verified for errors of omission (approximately 25 locations in each of the four image areas).

To measure errors of commission for cypress, 100 of the pixels classified as containing cypress were selected using a random cluster sampling technique. Five pixels classified as containing cypress were randomly selected in each of the four image areas. The four nearest pixels to each randomly selected pixel, that were classified as containing cypress, were also selected. Random cluster sampling was employed to reduce the areas of field verification to localized clusters. This same method was used to measure errors of commission for tupelo.

Field verification involved orientation with the TM grid overlaid on the 1:7,000-scale CIR aerial photographs and the hand-held Global Positioning System receiver. Due to a large abundance of natural ground reference features that were visible in the aerial photographs (for example, large tree crowns, canopy openings, and waterways), it was possible to identify the ground location of individual TM pixels with a reasonable level of certainty. If one or more cypress trees occurred within the estimated ground location of the TM pixel, it was recorded as a correctly classified cypress pixel. This method of determining the TM pixel ground locations was not precise enough, however, to permit the measurement of the amount of cypress or tupelo in each pixel. Additional details about the accuracy assessment are found in Karaska *et al.* (1995).

[2]Other government sponsored studies have quantified the AASAP procedure's ability to correctly estimate subpixel proportions (fractions) of materials of interest. For example, in one study several thousand panels were deployed in a variety of settings (open grass, open woodland, fallow field, morning, midday, wet, dry, clear, partly cloudy). The panels ranged in size from 0.05 to 4.0 pixels. They were deployed in a uniform grid pattern and grouped according to size. This allowed the sizes of detected panels to be identified based on their positions within the detected grid. The panels were bright relative to the background, allowing pixel brightness to be used as a measure of the relative fractions of a panel that fell in neighboring pixels for those targets that overlapped pixel boundaries. The study revealed a strong correlation ($r > 0.90$) of measured material pixel fractions with known panel sizes.

Results and Discussion

Approximately 75 percent of each of the four study areas was vegetated, and cypress and tupelo trees occupied approximately 20 to 30 percent of the vegetated regions. Subpixel classification results for tupelo wetland for one of the training areas are shown in Plate 1. The classified pixels are draped over a Landsat TM Band 4 image in various colors ranging from yellow through orange to green that represent the proportion (fraction) of tupelo found within each pixel (refer to inset table in Plate 1). For example, there were 365 pixels within this subscene that contained >90 percent tupelo. The location of these pixels corresponded to the location of dense stands of tupelo observed in the aerial photographs. Pixels with a high concentration of tupelo ran throughout the center of the region in a well defined wetland area. Pixels classified as containing a small amount of tupelo (< 30 percent) typically occurred in small isolated wetland areas. Although individual tupelo trees where often difficult to distinguish on the aerial photographs, the presence of some tupelo was identified in the immediate vicinity of these low fraction pixel locations. The reported fraction of tupelo and cypress in classified pixels was qualitatively compared to estimations of the amount of tupelo and cypress interpreted from the aerial photograph. Although some uncertainty existed in the determination of the presence and amount of cypress and tupelo trees, and in the precise location of the classified pixel on the aerial photograph, there was good agreement.

The error evaluation revealed that 95 of the 100 selected pixels classified as cypress contained cypress, and 93 of the 100 selected pixels classified as tupelo contained tupelo. Cypress thus had a 5 percent error of commission and tupelo had a 7 percent error of commission (Table 2). To evaluate

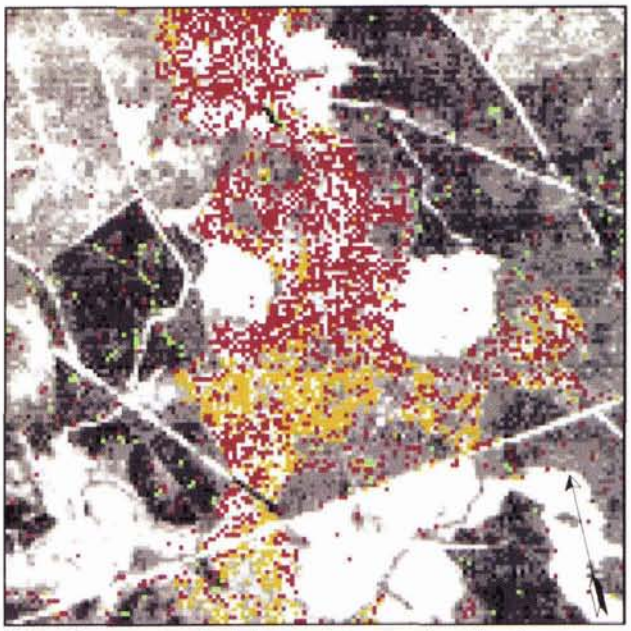

Plate 2. AASAP and minimum-distance classification results for cypress in one training area. Detections by AASAP only are in red. Detections by the minimum-distance classifier only are in green. Detections made by both AASAP and the minimum-distance classifier are in yellow. Much of the wetland area contained cypress mixed with other tree species and was only classified by AASAP.

TABLE 3. AASAP AND MINIMUM-DISTANCE CLASSIFICATION ACCURACY ASSESSMENT RESULTS

Class		AASAP	Minimum Distance
Tupelo	Total	91	85
	Commission	93/100	88/100
	Omission	89/100	81/100
Cypress	Total	89	71
	Commission	95/100	82/100
	Omission	82/100	59/100

errors of omission, ten stands of cypress and ten stands of tupelo in each of the four study areas were identified using the CIR photography and field verification. Five of these stands in each study area were randomly selected and five pixels within these selected stands were selected using stratified random sampling. For cypress, 82 of the 100 pixels (25 from each image area) known to contain cypress were successfully classified as cypress. For tupelo, 89 of the 100 known tupelo pixels were classified as tupelo. Table 2 lists the total accuracy for cypress, 89 percent (177/200), and tupelo, 91 percent (182/200).

Of the 182 pixels correctly classified as tupelo, all 182 sites contained tupelo trees mixed with other tree species. At most of these sites, the pixel area was predominantly occupied by tupelo (greater than 50 percent), but at some sites tupelo trees occupied less than 50 percent of the pixel area. In approximately a dozen of these sites, only a few tupelo trees occurred, representing as little as 20 percent of a pixel area. In evaluating the classification accuracy of tupelo in each of the four study areas, it was observed that the accuracy in each area was not significantly different. The accuracy in one training area was slightly better than in the other three areas, but no area had a total accuracy lower than 84 percent.

Based on this sample, it can be stated with 95 percent confidence that 93 percent ± 1.2 percent of all pixels classified as tupelo were correctly classified, and that 89 percent ± 1.2 percent of all areas containing tupelo were correctly classified. For cypress, also at the 95 percent confidence level, 95 percent ± 1.2 percent of all pixels classified as cypress were correct, and 82 percent, ± 1.3 percent of all areas containing cypress were correctly classified.

Table 3 lists the accuracy assessment results of cypress and tupelo for the AASAP and the minimum-distance classification. The AASAP classification performed 6 percent better than the minimum-distance classifier on tupelo and 18 percent better on cypress. For Tupelo, both the AASAP and the minimum-distance classifier performed well, 91 percent and 85 percent, respectively. The high minimum-distance tupelo classification results are due to several factors. Most importantly, the tupelo trees in this study area grew in clusters of several to many trees. Thus, most pixels containing tupelo contained a large amount of tupelo. The minimum-distance tupelo training set contained this high percentage tupelo mixture and thus did well in classifying most of the tupelo in the study area. Also important were the high quality *in situ* field data utilized for training in a study area that was well known.

For Cypress, AASAP performed 18 percent better than the minimum-distance classifier (89 percent versus 71 percent total accuracy). Cypress trees in this study area did not grow in clusters but typically occurred as isolated trees. The crown of individual cypress trees was typically < 30 m in diameter and therefore occurred in mixed pixels. Although mixed pixels of cypress were used in the training set, the minimum-distance classifier did not detect 41 percent of the cypress (59 percent omission accuracy). It is suspected that the mixture of cypress and other tree species in the training set pixels represented the more common mixtures, but there were other mixtures of tupelo with other tree species that were not represented in the training set. To classify these missed occurrences of tupelo, additional signatures would need to be developed. The AASAP signature detected more of the tupelo (82 percent omission accuracy) because its signature was of the pure tupelo, and it could detect subpixel occurrences of tupelo in pixels mixed with other materials.

Plate 2 depicts the AASAP and minimum-distance classification results of cypress for one of the 150- by 150-pixel training areas. A large wetland over 1 km in width runs north to south through this area. The yellow pixels are those classified by both processes. The green pixels were classified only by the minimum-distance classifier. Analysis of the aerial photographs revealed that a significant number of these locations (especially the isolated occurrences) probably did not contain cypress (18 percent of the minimum-distance classified pixels are errors of commission). The others represent a condition of tupelo that was not classified by AASAP (presumably not represented in the training set). The red pixels were pixels classified by AASAP and missed by the minimum-distance classifier, which had a 41 percent error of omission. Large areas of the wetland were detected only by AASAP. Aerial photography and field verification confirmed that almost all of these locations contained cypress mixed with varieties of other wetland hardwood tree species (AASAP cypress commission accuracy was 95 percent).

Conclusions

Spectral subpixel processing classified tupelo at 91 percent accuracy and cypress at 89 percent accuracy in Georgia and South Carolina wetlands. Extensive field investigation revealed that both tupelo and cypress trees were successfully classified when they occurred both as pure stands and as mixed stands. In an extensive comparison with traditional classifiers (ISODATA clustering, maximum likelihood, and minimum distance), the subpixel classifications of cypress and tupelo was significantly better. For cypress, AASAP performed 18 percent better and for tupelo 6 percent better than the best traditional classification results (minimum distance). Large areas of wetland, where cypress occurred heavily mixed with other tree species, were correctly classified by AASAP and not classified by the other classifiers.

The subpixel process can detect spectrally unique materials in most multispectral data sources. The process addresses the mixed-pixel problem and enables the classification of materials smaller than the spatial resolution of the sensor by (1) extracting a pure subpixel signature of the material of interest (units of the pixel that are not the material of interest are removed from the signature), and (2) extracting and analyzing subpixel components of each pixel in an image and identifying those subpixel components that match the material-of-interest spectral signature. While the analyst could use a library of pre-existing spectral signatures, the algorithm presented here provides the analyst with a signature development capability that produces signatures tailored to a specific material of interest in the study area with its unique environmental conditions.

The improved accuracy of wetland species classification should allow Thematic Mapper and other multispectral data sources to more reliably support field operations in forested wetlands mapping. Although the satellite imagery will not replace field work or even the use of aerial photographs, it can potentially reduce the required area of coverage for the field work and photo interpretation efforts. The AASAP approach to classifying materials in mixed pixels is new and unique. The ability to classify individual tree and plant spe-

cies and report the amount of the species in each pixel has the potential to benefit many other diverse wetland, forestry, agriculture, and ecological applications.

Ackowledgments

This research was funded in part by NASA's Earth Observation Commercial Application Program (EOCAP), Stennis Space Center, Mississippi.

References

Adams, J.B., M.O. Smith, and P.E. Johnston, 1986. Spectral Mixture Modeling: A New Analysis of Rock and Soil Types at the Viking Lander I Site, *Journal of Geophysical Research*, 91:8098–8112.

Ewel, K.C., 1990. Multiple Demands on Wetlands; Florida Cypress Swamps can Serve as a Case Study, *Bioscience*, 40(9):660–666.

Hodgson, M.E., J.R. Jensen, H.E. Mackey, and M.C. Coulter, 1988. Monitoring Wood Stock Foraging Habitat Using Remote Sensing and Geographic Information Systems, *Photogrammetric Engineering & Remote Sensing*, 54(11):1601–1607.

Huguenin, R.L., 1994. Subpixel Analysis Process Improves Accuracy of Multispectral Classifications, *Earth Observation Magazine*, 3(7):37–40.

Jensen, J.R., 1996. *Introductory Digital Image Processing: A Remote Sensing Perspective*, Second Edition, Prentice-Hall, Inc., Englewood Cliffs, New Jersey, 318 p.

Jensen, J.R., K. Rutchey, M. Koch, and S. Narumalani, 1995. Inland Wetland Change Detection in the Everglades Water Conservation Area 2A Using a Time Series of Normalized Remotely Sensed Data, *Photogrammetric Engineering & Remote Sensing*, 61(2): 199–209.

Karaska, M.A., R.L. Huguenin, D. Van Blaricom, and B. Savitsky, 1995. Subpixel Classification of Cypress and Tupelo Trees in TM Imagery, *Technical Papers of the American Society for Photogrammetry & Remote Sensing*, Charlotte, North Carolina, pp. 856–865.

Smith, M.O., S.L. Ustin, J.B. Adams, and A.R. Gillespie, 1990. Vegetation in Deserts: I. A Regional Measure of Abundance from Multispectral Images, *Remote Sensing of Environment*, 31:1–26.

Wang, F., 1990a. Improving Remote Sensing Image Analysis through Fuzzy Information Representation, *Photogrammetric Engineering & Remote Sensing*, 56(8):1163–1169.

———, 1990b. Fuzzy Supervised Classification of Remote Sensing Images, *IEEE Transactions on Geoscience and Remote Sensing*, 28(2):194–201.

(Received 3 June 1996; accepted 12 September 1996; revised 1 January 1997)

Forthcoming Articles

Peter M. Atkinson and Paul J. Curran, Choosing an Appropriate Spatial Resolution for Remote Sensing Investigations.

Georges Blaha, Accuracy of Plates Calibrated by an Automatic Monocomparator.

Michel Boulianne, Clément Nolette, Jean-Paul Agnard, and Martin Brindamour, Hemispherical Photographs Used for Mapping Confined Spaces.

Roland J. Duhaime, Peter V. August, and William R. Wright, Automated Vegetation Mapping Using Digital Orthophotography.

Gary R. Clay and Stuart E. Marsh, Spectral Analysis for Articulating Scenic Color Changes in a Coniferous Landscape.

Clyde C. Goad and Ming Yang, A New Approach to Precision Airborne GPS Positioning for Photogrammetry.

Kazuo Kobayashi and Chuji Mori, Relations between the Coefficients in Projective Transformation Equations and the Orientation Elements of a Photograph.

Rongxing Li, Mobile Mapping — An Emerging Technology for Spatial Data Acquisition.

D.D. Lichti and M.A. Chapman, Constrained FEM Self-Calibration.

Hans-Gerd Maas and Thomas Kersten, Aerotriangula-tion and DEM/Orthophoto Generation from High Resolution Still-Video Imagery.

Scott Mason, Heuristic Reasoning Strategy for Automated Sensor Placement.

Paul Sutton, Dar Roberts, Chris Elvidge, and Henk Meij, A Comparison of Nighttime Satellite Imagery and Population Density for the Continental United States.

J.E. Vogelmann, T. Sohl, and S.M. Howard, Regional Characterization of Land Cover Using Multiple Sources of Data.

Timothy A. Warner and Michael Shank, An Evaluation of the Potential for Fuzzy Classification of Multispectral Data Using Artificial Neural Networks.

July Issue — Landsat 25th Anniversary

Donald T. Lauer, Stanley A. Morain, and Vincent V. Salomonson, The Landsat Program: Its Origins, Evolution, and Impacts.

Aram M. Mika, Three Decades of Landsat Instruments.

K. Thome, B. Markham, J. Barker, P. Slater, and S. Biggar, Radiometric Calibration of Landsat.

David Landgrebe, The Evolution of Landsat Data Analysis.

William C. Draeger, Thomas M. Holm, Donald T. Lauer, and R.J. Thompson, The Availability of Landsat Data: Past, Present, and Future.

Ray A. Williamson, The Landsat Legacy: Remote Sensing Policy and the Development of Commercial Remote Sensing.

Samuel N. Goward and Darrel L. Williams, Landsat and Earth Systems Science: Development of Terrestrial Monitoring.

Stephen G. Ungar, Technologies for Future Landsat Missions.